Research Article

Improvement of Experimental Equipment Based on the One-Step Outflow Test and Research on Rapid Determining SWCC

Jiaqi Wu [ID],[1] **Huan Li,**[1] **Anming Wang,**[1] **and Zhiquan Huang** [ID][2]

[1]*College of Geosciences and Engineering, North China University of Water Resources and Electric Power,*
 Zhengzhou 450046, China
[2]*Luoyang Institute of Science and Technology, Luoyang 471023, China*

Correspondence should be addressed to Zhiquan Huang; huangzhiquan@ncwu.edu.cn

The soil-water characteristic curve (SWCC) is an important hydraulic parameter for modeling water flow and contaminant transport in the unsaturated soil. However, direct measurement of the SWCC is still difficult. The commonly used measuring instrument in the laboratory is the pressure plate extractor. In this paper, the original pressure plate extractor has been improved based on the one-step outflow test. Compared with the original pressure plate extractor, three devices, water storage, data acquisition system, and bubbles scouring device, are added to the improved pressure plate extractor. The improved equipment eliminates the problems of long test time consumption and inaccurate test data. A one-step outflow test is performed utilizing the improved pressure plate extractor. The test data (the amount of spilled water and the time of pressurization) are substituted into the one-dimensional moisture migration analysis software HYDRUS-1D. The parameters (α, m, and n) are identified by the numerical inversion method in the inversion module of the HYDRUS-1D, which are associated with the VG model to fit SWCC. The fitted SWCC is highly consistent with the measured SWCC, which is obtained from the conventional test of the original pressure plate extractor. Results confirm that the improved pressure plate extractor not only saves considerable time but also effectively measures the SWCC. The improved pressure plate extractor also involves a simple operation. The influence factors of controlling the geometry of SWCC are also discussed, the results of the discussion confirm that the geometry of SWCC is directly controlled by pore distribution, and the consolidation pressure is an indirect factor.

1. Introduction

Knowledge of infiltration characteristics is necessary for hydrological studies in different soils [1]. The soil-water characteristic curve (SWCC) reflects the process of water entering the soil, which presents the relationship between the matrix suction and water content (such as saturation or volumetric water content). The hydraulic conductivity function [2, 3], volumetric variation of the soil [4–7], shear strength in the unsaturated soil [8, 9], and attributes of the water content in the subsurface [10–13] can be computed using the SWCC. This relationship plays an important role in the research and practical engineering related to unsaturated soils. A pressure plate extractor is commonly used to measure the SWCC in the laboratory. Two methods are usually adopted [14, 15]: the weighing soil method

(WSM), which measures the water content by weighing the sample when equilibrium is reached, and the weighing outflow method (WOM), which measures the water content by weighing the amount of spilled water from the sample after equilibrium is attained. In the WSM, some soil particles may be lost, meaning that the measured value is less than the actual value. In the WOM, due to high pressure and a long testing time, bubbles are accumulated on the back of the ceramic plate, and water is occupied by bubbles; thus the water is pushed out, and the amount of spilled water is overestimated. There are errors in both methods. Therefore, determining the SWCC quickly and accurately is a key problem to be solved.

Many scholars have conducted in-depth and extensive research on rapid determination of the SWCC. Ng and Peng [16] measured the SWCC of residual soil in Hong Kong

under K_0 state by using an improved volume pressure plate device. Lu et al. [15] presented a constant flow laboratory testing method (CFM) for concurrently measuring the SWCC and hydraulic conductivity function (HCF) of unsaturated coarse-grained soils. Chen et al. [17] determined the SWCC of silt quickly and accurately by using a combined system for the concurrent measurement of the hydraulic properties of unsaturated soils. The results were compared with the SWCC obtained by the adjusted WOM, confirming the usability and effectiveness of the combined system. Yi et al. [18] refitted the pressure chamber of the combined system with a constant flow method and additional equipment to scour and weigh the air bubbles at the bottom of the ceramic plate. After refitting, the one-step and multistep outflow tests were conducted to accurately and rapidly measure the SWCC of silt. Wang and Linc [19] used a pressure plate extractor and GDS unsaturated triaxial apparatus to study the influencing factors, such as types of soil and net mean stress, using the Fredlund five-parameter model through least squares to fit the SWCCs. Lee et al. [20] introduced an improved automatic flow pump system, which measured the transient suction response by using the balance method during the drying and wetting cycles to obtain the soil-water retention curve (SWRC). Dong and Dong [21] established twin-cake testing, which is a new method based on the drying cake method, to measure suction-stress characteristic curve (SSCC) under drying and wetting conditions. The results demonstrated that the new testing system provides a simple, fast, and nondestructive way to measure SSCC under various conditions. An improved pressure plate extractor with an evaporation compensation system [22] has been developed to measure the transient water content curve of soil in multistep outflow tests. This direct measurement method describes the change in hydraulic conductivity during each step. Rahardjo et al. [23] combined a centrifuge and a chilled mirror psychrometer to find a rapid and reliable technique to obtain the SWCC for a large range of suctions. A comparison of this technique with the axis translation method showed that the SWCC determined using the former agreed well with those determined using the latter. The elapsed time was also reduced from a few months for the axis translation method to two days for the combined centrifuge and chilled mirror psychrometer. Adel et al. [24] developed a novel automatic system that adopts the continuous pressurization method and allows the direct determination of the SWCC in a short time suitable for use with remolded and undisturbed samples. Zhao et al. [25] proposed a novel simplified equation based on the van Genuchten model, whereby SWCC hysteresis can be easily predicted from the initial drying SWCC. Zheng et al. [26] proposed a void-ratio-dependent shear strength model, incorporating the influence of the change in void ratio on the SWRC pattern. The model is validated against the experimental data from the tests. Ng and Pang [27] studied the SWCC of remolded soil and natural soil, and the results show that the SWCC of a remolded sample is very different from that of a natural sample with the same initial soil density and initial water content. When the remolded sample is subjected to different stress states, its structure and SWCC will change greatly. Sun et al. [28] studied the collapsibility characteristics of unsaturated compacted clay with different initial dry density and suction, and it is found that the SWCC in terms of suction and degree of saturation shifts upwards with increasing specimen density. The SWCC of a compacted soil mainly depends upon the current density, not directly upon the stress state. Salager et al. [29] comprehensively demonstrated that the soil-water retention curves (SWRCs) obtained are synthesized and compared in terms of water content, void ratio, and degree of saturation, and the void ratio is noticed to exert a clear influence on the SWCC. All the above scholars are working hard for the accurate and rapid determination of SWCC. Zhai et al. [30] developed a framework in which different SWCCs in the form of saturation are generated based on the measured SWCCs in the form of gravimetric water content of soil in a relatively loose condition and the volumetric shrinkage curve. The proposed framework is based on the concept of the pore size distribution function. The estimated SWCCs corresponding to different initial void ratios from the proposed framework were verified by using experimental data from published studies. After reading literature, the authors have an idea, which will be introduced in detail later.

In this paper, the one-dimensional stress controllable volumetric pressure plate extractor (1D-SDSWCC) is improved. A one-step outflow test was performed in the silt by the improved pressure plate extractor, and a one-dimensional water transport model is established in HYDRUS-1D. According to the test data (the amount of spilled water and the time of pressurization) and model, SWCC is fitted quickly and effectively. The SWCC measured by the original pressure plate extractor is defined as measured SWCC, and the SWCC measured by the improved pressure plate extractor is defined as fitted SWCC. The two curves almost coincide, which not only verifies the reliability and practicability of the improved pressure plate extractor but also proves the rapidity and convenience of the one-step outflow method. Because the pressure is too high during the test, the influence of consolidation pressure on SWCC is discussed.

The aim and innovation of the paper are to improve the original pressure plate extractor which does not meet the one-step outflow test, so that the improved pressure plate extractor can meet the requirements of one-step outflow test, and an experimental research is carried out, to achieve the purpose of obtaining the SWCC of silt quickly and effectively, and then influence factors of controlling the geometry of SWCC are also discussed; the result states that the pore distribution of sample is a direct factor that affects the geometry of SWCC, which is changed by the consolidation pressure to affect the geometry of SWCC.

2. Mathematical Model

HYDRUS-1D is a numerical simulation software to simulate the one-dimensional outflow, solute, and heat transfer [31]. In this paper, inverse solution in HYDRUS-1D is used to optimize the soil-water characteristic parameters. When the parameters of the soil-water characteristic curve are

estimated by the numerical inversion method [32] in the inverse module, the water content and unsaturated hydraulic conductivity are represented by equations containing finite independent variables (e.g., α, n, θs, θr, and l of the VG model), these independent variables are given the initial estimation value and error range (setting the maximum and minimum range of parameter optimization) to form the function expression of h and $K(h)$, and then the optimized parameters are substituted into the moisture equation of VG model; combined with the initial and boundary conditions in the test, a comprehensive mathematical equation to describe the soil-water movement was formed. Then the soil-water characteristic parameters are obtained by solving the water movement equation, and the water content was calculated by unsaturated water equation and compared with the experimental data. Then, the parameters are improved according to the set interval of the maximum value and minimum value, and the iterative calculation is repeated until the error between the numerical simulation results and the test results is minimized. Subsequently, the set parameter value is the optimized inversion value.

The state of moisture movement in soil is fully described by the mathematical equations in HYDRUS-1D. Combined with the test data (the amount of spilled water and the time of pressurization), iterative calculation was repeated, and then the optimal characteristic parameters (α, m, and n) were obtained by solving the moisture movement equation. The optimal soil-water characteristic parameters were substituted into VG model to fit SWCC.

2.1. Basic Equations for Model in HYDRUS-1D.
The moisture in the silt sample moves from top to bottom during the test. Thus, only the one-dimensional soil moisture infiltration problem is considered in the test. The moisture is isotropic in soil. Richards' equation is chosen to describe the variation rule of moisture transport in the soil profile as follows:

$$\frac{\partial \theta(h)}{\partial t} = \frac{\partial}{\partial z}\left[K(h)\frac{\partial h}{\partial z} + K(h) \right], \tag{1}$$

where θ is the volume of the water content, K is the hydraulic permeability function, h is the pressure head, and t is time.

2.2. Soil-Water Characteristic Curve.
In equation (1), $\theta(h)$ is the SWCC of the unsaturated soil, which has a nonlinear relationship with h. Thus, the parameters (α, m, and n) in

equation (1) are difficult to determine. The VG model is selected to describe the SWCC in HYDRUS-1D as follows:

$$\theta(h) = \begin{cases} \theta_r + \dfrac{\theta_s - \theta_r}{[1 + |\alpha h|^n]^m}, & h < 0, \\[3mm] \theta_s, & h \geq 0, \end{cases} \tag{2}$$

where θs is the saturated volumetric water content, θr is the residual volumetric water content, and α, m, and n are empirical parameters.

2.3. Initial/Boundary Conditions of the Model.
P_0 is the initial value condition of the model:

$$h = h_0(x) + l, \quad t = 0, \ 0 \leq x \leq H,$$
$$h_0 = \frac{p_0}{\rho g}, \tag{3}$$

where l is the height difference between the bottom of the sample and the water surface in the cup. The bottom of the sample is generally higher than the water surface in the cup.

The upper boundary flow is constant at 0. Thus, the flow Q can be regarded as zero and can be represented as follows:

$$Q = 0,$$
$$t > 0, \tag{4}$$
$$x = H.$$

The lower boundary is the pressure boundary, expressed by the pressure head h:

$$h = h(t),$$
$$t > 0, \tag{5}$$
$$x = 0,$$

where $h(t)$ refers to h at the bottom boundary of the sample (which can be converted from the pressure to h).

2.4. Numerical Solution of the Model

2.4.1. Dispersion of Space and Time.
The soil profile is divided into several continuous cell cubes, which are the nodes in the end. The total number of nodes is N. Equation (1) is discretized, and the finite difference scheme is as follows:

$$\frac{\theta_i^{i+1,k+1} - \theta_i^j}{\Delta t} = \frac{1}{\Delta x}\left(K_{i+(1/2)}^{j+1} - h_i^{j+1,k+1} - K_{i-(1/2)}^{i+1k} \frac{h_i^{j+1,k+1} - h_{i-1}^{j+1,k+1}}{\Delta x_i} \right) + \frac{K_{i+(1/2)}^{j+1,k+1} - K_{i-(1/2)}^{j+1,k}}{\Delta x}\cos \alpha, \tag{6}$$

where $i-1$, i, and $i+1$ are the positions in the finite difference grid; k and $k+1$ are the previous and current

iteration steps, respectively; and j and $j+1$ are the previous and current time steps, respectively.

When equation (6) is solved, the method of Taylor expansion, as proposed by Celia et al (1990), is adopted as follows:

$$\frac{\theta_i^{j+1,k+1} - \theta_i^j}{\Delta t} = C_i^{j+1,k} \frac{h_i^{j+1,k+1} - h_i^{j+1,k}}{\Delta t} + \frac{\theta_i^{j+1,k} - \theta_i^j}{\Delta t}, \tag{7}$$

$$C_i^{j+1,k} = \frac{d\theta}{dh}|^{j+1,k}. \tag{8}$$

The above method can minimize iteration error and subsequently obtain a better result. The second term on the right side of equation (7) is known in the current iteration step. The first term on the right side of equation (7) converges to zero at the end of the iteration.

2.4.2. Parameter Optimization Estimation.

The optimized parameter is obtained after minimizing the objective function. During parameter optimization, the objective function in the moisture migration analysis model of HYDRUS-1D is as follows:

$$\phi(b, q, p) = \sum_{j=1}^{m} v_j \sum_{i=1}^{n_{qj}} \omega_{i,j} \left[q_j^*(x, t_i) - q_i(x, t_i, b) \right]^2$$
$$+ \sum_{j=1}^{m_p} \overline{v}_i \sum_{i=1}^{n_{pj}} \overline{\omega}_{i,j} \left[p_j^*(\theta_i) - p_i(\theta_i, b) \right]^2 + \sum_{j=1}^{n_b} \overline{v}_i \left[b_j^* - b_i \right]^2. \tag{9}$$

From equation (9), the objective function in HYDRUS-1D includes the water content and water characteristic function of the sample. This function contains more information compared to the previous inversion objective function, and the accuracy of parameter inversion is improved.

3. Introduction of Instruments

3.1. Original Pressure Plate Extractor.

The original instrument is the 1D-SDSWCC (Figure 1), which mainly consists of three parts: the control panel, the pressure chamber, and the water volume measurement system.

(1) The control panel is composed of an air compressor and a pressure regulating panel. The main purpose is to adjust the pressure in the pressure chamber. Stable and constant pressure is supplied to the instrument during the entire test.

(2) The pressure chamber is cylindrical. During the test, the sample is put into the pressure chamber and the pressure chamber is sealed.

(3) The water volume measurement system is on the surface of the pressure regulating plate. Before the test, the water is fed into two glass tubes, and the position of the water in the glass tubes is recorded. After the experiment, the pressure chamber is pressurized, and the water in the sample flows into the glass tube on the left. When the difference in water levels in the two tubes does not change, the
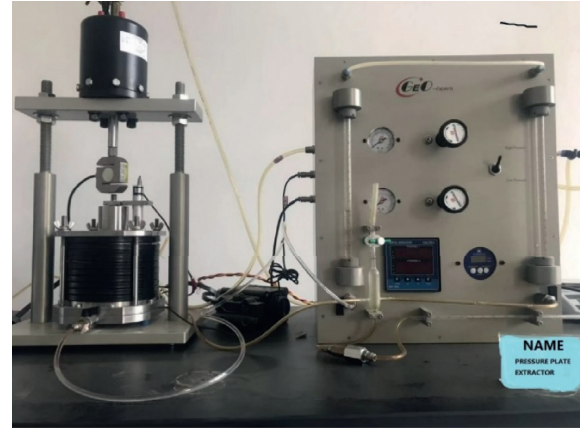

FIGURE 1: Original pressure plate extractor.

sample has reached the equilibrium state (the amount of outflow in the sample does not change). By repeating the above steps, the corresponding water content of the sample under different pressures can be obtained. Thus, an SWCC can be obtained.

The test principle of the original pressure plate extractor is axis translation technology. By increasing the pore gas pressure (u_a), the pore water pressure (u_w) is changed from the negative value of the natural state to a certain value, achieving the matrix suction measurement. Measurement of the SWCC by using the conventional test with the pressure plate extractor typically takes a long time, approximately 1.5–6 months.

Three defects in the one-step outflow test on the original pressure plate extractor are observed as follows:

(1) Two relationships are required in the one-step outflow test: One is the relationship between the loading pressure and compression time, and the other is the relationship between the amount of spilled water and the compression time in the one-step outflow test which cannot be monitored.

(2) Although the water volume measurement system reduces the operation of taking out sample for weighing, owing to the long test time, the bubbles will be separated on the back of the ceramic plate. These bubbles occupy the position of the water at the bottom of the ceramic plate, causing the amount of spilled water to be large (the difference between the mass obtained by taking out the sample for weighting and that obtained in the water volume measurement system is about 1.2–1.8 g). Therefore, the data from the water volume measurement system are not accurate during the test, and the measured water content is less than the real water content.

(3) Bubbles at the bottom of the ceramic plate are scoured by water during the test. When the original pressure plate extractor performs tests, the bubbles are scoured manually after the pressure of each stage reaches equilibrium. The scouring times are

numerous, and the operation is tedious. Bubbles are produced in one-step outflow test and must be scoured during the test. The purpose is to prevent water at the bottom of the ceramic plate being squeezed out by bubbles, because if the water is squeezed out by bubbles, the amount of spilled water in the test will be greater than the actual amount of spilled water. Obviously, the original pressure plate extractor cannot meet the requirement of scoured bubbles during the one-step outflow test.

3.2. Improved Pressure Plate Extractor.

Owing to the above three reasons, the requirements of the one-step outflow test are not satisfied by the original pressure plate extractor. Based on the original pressure plate extractor, three parts were added to the improved pressure plate extractor, namely, a water storage pipe, data acquisition system, and vacuum pump. The improved pressure plate extractor is shown as a sketch and a photograph in Figures 2 and 3, respectively.

The main parts of the improved pressure plate extractor are as follows:

(1) The control panel is composed of an air compressor, a pressure regulating button, and a pressure regulating panel. Indoor air is compressed to a high-pressure state by an air compressor, which provides the required pressure for the entire experimental instrument. The loading pressure value is precisely adjusted by the pressure regulating panel so that the pressure chamber can reach the target pressure value.

(2) The pressure chamber is composed of upper and lower cover plates. The ceramic plate is equipped on the lower cover plate. The pressure chamber is completely sealed during the test to avoid errors caused by air leaks.

(3) The pipeline is connected to the upper and lower portions of the water storage device. The upper pipeline is connected to the vacuum pump, and the lower pipeline is connected to the pressure chamber. The pipeline stores the entire tube of water for bubble scouring and pipeline saturation. The vacuum pump pumps water from the external storage device when the water in the storage pipe is insufficient. Thus, the water in the storage pipe is sufficient to ensure that the entire instrument can be scoured and the pipeline can be saturated.

(4) The weighing system consists of a high-precision electronic balance and a water cup with a small hole above it, which helps prevent moisture volatilization.

(5) The data acquisition system relates to the electronic balance, which is connected to the data acquisition software. The system collects the change data of the moisture spillage in the sample after the pressure is loaded. The time interval of the data of acquisition can be adjusted in the acquisition software as needed for the experiment.

Because the fine particles in clay have strong water-retaining capacity, the pressure required for the one-step outflow test is extremely high and consumes large amounts of time, which will lead to sample deformation and further affect the test results. Therefore, the improved pressure plate extractor in this paper only carries out the one-step outflow test on silt.

3.3. Comparison of Two Test Instruments

(1) The improved pressure plate extractor greatly reduces the test time to 90% less than that with the original pressure plate extractor.

(2) The improved pressure plate extractor can measure the SWCC only by loading the pressure once in the test, resulting in simple and convenient operation.

(3) During the experiment with the improved pressure plate extractor, the bubbles on the back of the ceramic plate are scoured by the vacuum pump, not only reducing the required manpower but also reducing errors between actual water content and measured water content.

(4) In the improved pressure plate extractor, the sample does not need to be removed from the pressure chamber for weighing. Thus, the test error is reduced.

4. Test Procedure

4.1. Test Procedure of the Conventional Test.

The conventional test was performed using the original pressure plate extractor. We referred to the test procedure in the work of Wang and Benson [33]. The main steps were as follows:

(1) *Sample Preparation.* According to the initial dry density and initial water content of the test design, the quality of the silt for the test is calculated. Then, the sample of ring knife is prepared. The ring knife has a diameter of 6.18 cm and a height of 2 cm.

(2) Before the test, the sample and instrument are saturated.

(3) *Loading Pressure.* The saturated sample is placed in the pressure chamber, and the pressure is applied as shown in Table 1.

(4) *Determination of the SWCC.* When the suction of each stage reaches equilibrium (the amount of spillover water in the sample does not change), the sample is removed from the pressure chamber and weighed. The corresponding water content is calculated in the equilibrium state. Thus, the SWCC of the sample can be obtained by repeated operation. The SWCC is shown in Figure 4.

(5) *Calculation of the Test Time.* In the test, the average time for each stage of the suction to reach equilibrium was 4 days. According to the application of the load suction in Table 1, 45 days are needed for the SWCC of the silt sample.
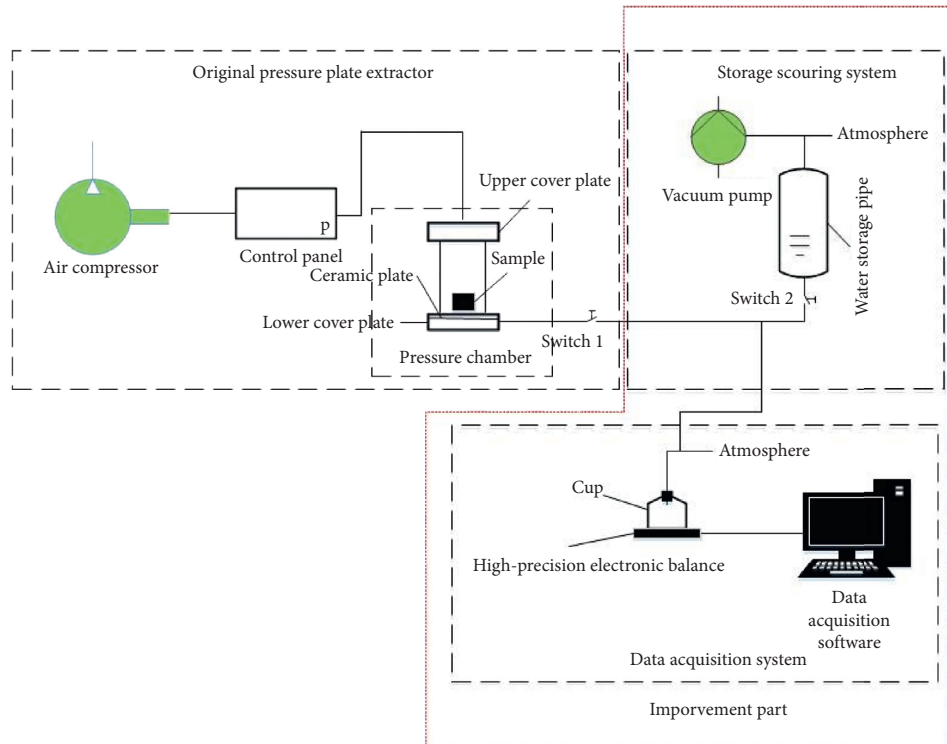
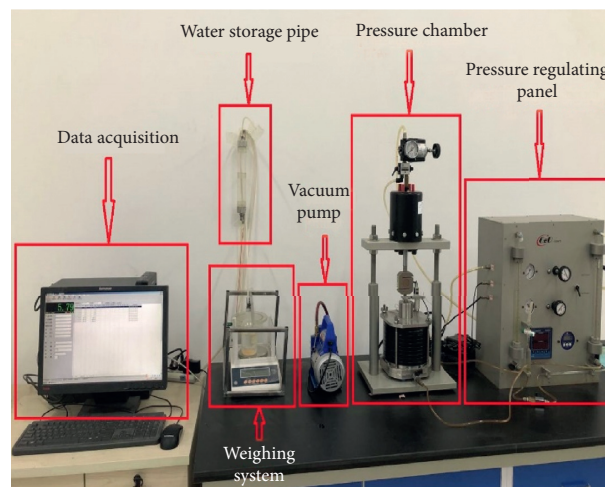Figure 2: Sketch of the improved pressure plate extractor.

Figure 3: Photograph of the improved pressure plate extractor.

Table 1: Suction paths.

Initial dry density	Suction paths
1.78 g/cm³	0 kPa⟶20 kPa⟶40 kPa⟶60 kPa⟶80 kPa⟶100 kPa⟶120 kPa⟶140 kPa⟶160 kPa⟶180 kPa⟶200 kPa

This test is a conventional test with several operational disadvantages. First, the test involves many steps, possibly facilitating the commission of errors. Second, during the test, sample weighing not only increases the test operation steps but also causes erroneous test results due to falling off the soil particles. Third, the conventional test requires a long time, and the bubbles are separated at the bottom of the ceramic plate. Bubbles occupy the position of the water, the water is squeezed out by bubbles from the bottom of the ceramic plate, and the amount of the spilled water is increased.
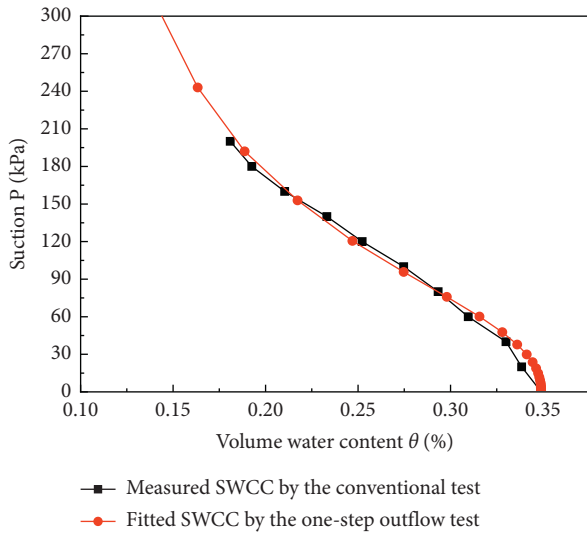
Figure 4: Comparison of measured SWCC and fitted SWCC.

4.2. Test Scheme of the One-Step Outflow Test. Silt with a dry density of 1.78 g/cm^3 was selected for the one-step outflow test. The test operation steps of the improved pressure plate extractor are briefly described as follows:

(1) The sample is prepared according to the conventional test sample-making process.

(2) The sample and ceramic plate are saturated.

    The sample is saturated by the vacuum saturation method. The sample is silt, so the vacuum device requires 3–4 h to off-gas. Then, the intake valve on the lid of the barrel is opened to let water into the barrel. To enable 100% saturation of the sample, the water intake in the barrel is adjusted thrice to saturate the sample. The time interval of each pumping is 1 h to sufficiently pump out the dissolved gas in the water.

    The ceramic plate is saturated according to the operation steps of the pressure plate extractor. First, air-free water is added to the pressure chamber, and the surface of the ceramic plate is submerged. Second, the valves on both sides of the base of the pressure chamber are opened, and all pipelines of the instrument are filled with water to saturate the pipeline. Third, through the adjustment of the pressure control panel, pressure (5 bar, because the air-entry value of the ceramic plate is 5 bar) is applied to the pressure chamber. The valve is closed for at least 8 h after it is drained for 1 h. Finally, the bubbles in the pipeline of the whole instrument are scoured until no bubbles are observed.

(3) The pipeline of the instrument is saturated. All pipelines are scoured by adjusting the switch of the valve until all bubbles in the pipeline are removed.

(4) The sample is loaded. The saturated sample is placed on the ceramic plate of the pressure chamber. The pressure chamber is sealed during the test.

(5) The relationship between the volume water content and time of the loading pressure is measured.

Prior to the test, the water in the storage pipe can enter the bottom of the ceramic plate by adjusting the valve. The bottom of the ceramic plate is scoured, and the bubbles in the bottom of the ceramic plate are discharged. Then, the data acquisition software is executed. Finally, a pressure of 290 kPa is applied in the sample until the amount of spilled water does not change. Hence, the amount of the spilled water is obtained at any time, and the relationship between the volume water content and time of loading pressure is obtained as $\theta(t)$.

5. Verification

5.1. Curve of θ–t. We performed the one-step outflow test using the improved pressure plate extractor. Silt was selected as the test sample. The initial dry density of the test sample was set to 1.78 g/cm^3. The basic physical index and particle composition were analyzed after drying, crushing, and sieving (Figure 5).

According to the amount of the spillover water, the volume water content of the sample was calculated. The relationship between the volume water content and the time of loading pressure was obtained in Figure 6. There are two curves in Figure 6: one is the curve of pressurization and the time of pressurization, and the other is the curve of the amount spilled water and the time of pressurization. Then, the curve of the amount of spillover water and the time of pressurization was fitted (in Figure 7) based on the curve of θ–t, the initial/boundary conditions, and the 1D moisture migration model. It can be seen from Figure 7 that the data fitted by the 1D moisture migration model are basically consistent with the data measured by the improved pressure plate extractor. The high coincidence between fitted data and measured data proves that the solution of moisture movement equation reaches the optimal solution and the optimal parameters can be solved at this time. The optimal characteristic parameters in the VG model are shown in Table 2.

5.2. Comparison of Two SWCCs. The optimal characteristic parameters in Table 2 were substituted into the VG model to fit SWCC. The SWCC measured by the conventional test with the original pressure plate extractor is called the measured SWCC, whereas the SWCC measured by the proposed method is called the fitted SWCC. The two SWCCs are visualized in the same picture for analysis and comparison (Figure 4). The fitted and measured SWCCs are almost consistent. Therefore, the one-step outflow test can estimate the SWCC. The conventional test with the pressure plate extractor to determine SWCC uses the axis-translation method. In this paper, the conventional test with the original pressure plate extractor requires 45 days to determine the SWCC. By contrast, the one-step outflow test with the improved pressure plate extractor only requires 4.5 days to determine the SWCC. A diagram of the times consumed by the two tests is shown in Figure 8. The one-step outflow test
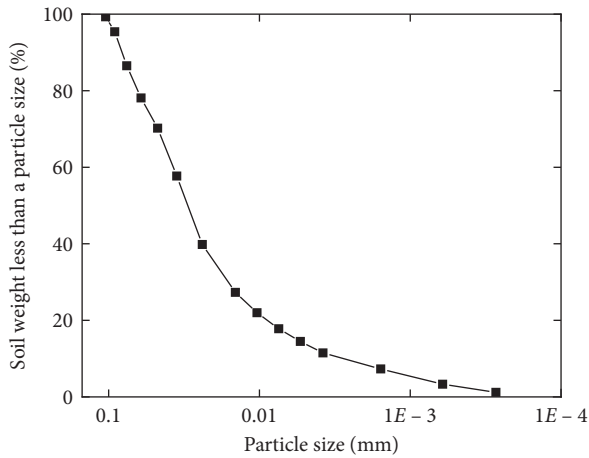
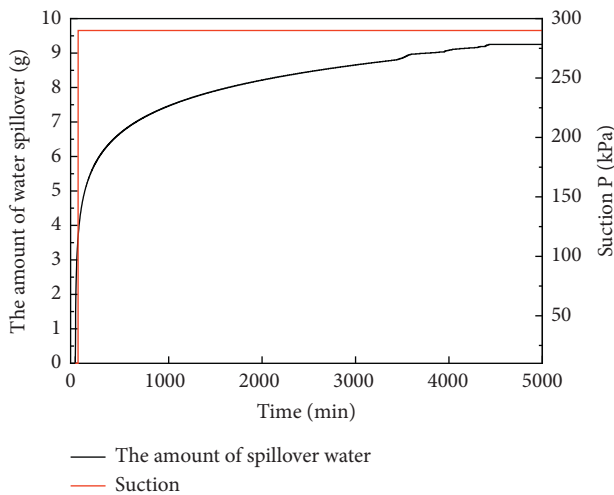FIGURE 5: Grain size distribution of tested sample.

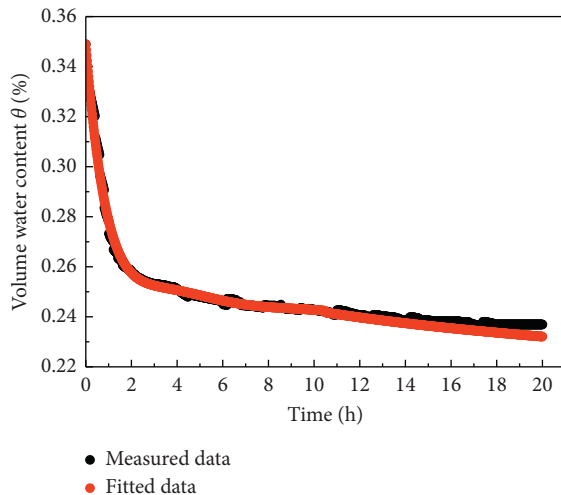FIGURE 6: Curves of outflow and suction with time.

FIGURE 7: Curve of volume water content and time.

TABLE 2: Optimal characteristic parameters.

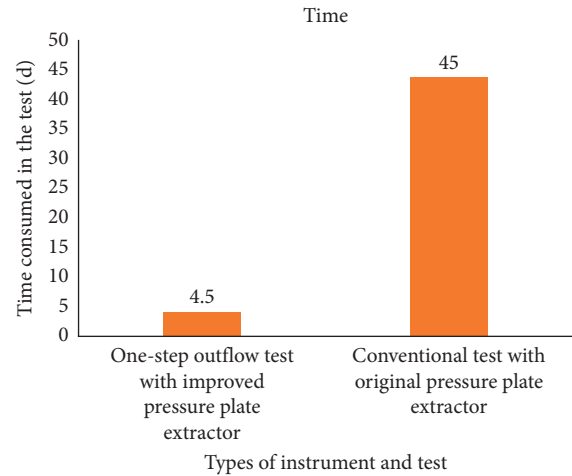| Model parameters				
A (cm^{-1})	n	m	θr	θs
0.0009	2.29	0.56	0.073	0.349

FIGURE 8: Test duration comparison.

requires 40.5 days less to determine the SWCC and can quickly and effectively determine the SWCC of silt.

6. Influence of Consolidation on the SWCC

Many experimental studies show that many factors affect the geometry of SWCC, including mineral composition, particle structure, pore size distribution, sample preparation method, stress state, stress history, and density (initial void ratio). Many scholars are devoted to studying the influence of changes of pore ratio on SWCC. Sun et al. [28] and Gallipoli et al. [34] found through data analysis or tests that the decisive factor affecting the SWCC is the void ratio, while the stress state indirectly affects the SWCC by changing the pore size distribution (void ratio) of the soil. In this experiment, the excessive loading pressure leads to the consolidation of the sample during the test. Does consolidation affect SWCC? This question is discussed in the paper. The consolidation test increased the dry density of the silt sample from 1.65 g/cm^3 to 1.78 g/cm^3. Then, the conventional and one-step outflow tests of the consolidated sample were carried out, and the results were compared and analyzed. The sample of silt with a dry density of 1.65 g/cm^3 was prepared using a large ring cutter with a diameter of 9 cm and a height of 4 cm. The preparation procedure was the same as that of the silt sample with an initial dry density of 1.78 g/cm^3. After the sample is saturated, the consolidation test is carried out. The dry density of the sample increased from 1.65 g/cm^3 to 1.78 g/cm^3. Finally, a small ring cutter with a diameter of 6.18 cm and a height of 2 cm was used to cut a small ring cutter sample from the consolidated sample. This small sample is used for the conventional test and the one-step outflow test.
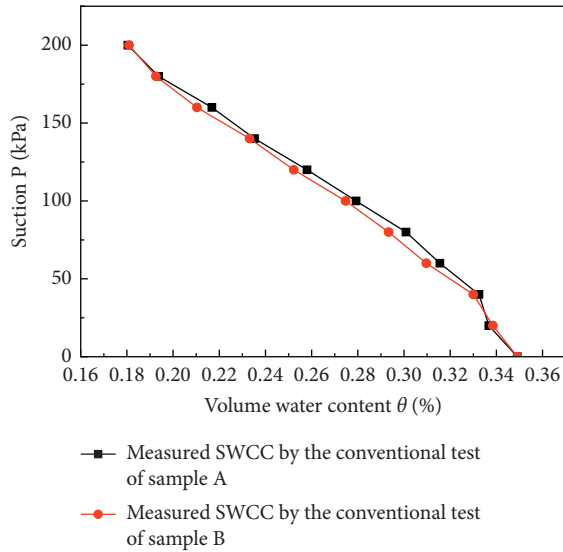
FIGURE 9: Comparison of Sample A with Sample B of SWCC measured by conventional test.

6.1. Comparison of Measured SWCC by the Conventional Test after Consolidation.

The dry density of the sample increased from $1.65\,g/cm^3$ to $1.78\,g/cm^3$ and is marked as Sample A. The samples with an initial dry density of $1.78\,g/cm^3$ are marked as Sample B. The conventional tests are carried out on Sample A and Sample B, and two measured SWCCs can be obtained, which are measured, analyzed, and compared as shown in Figure 9.

In Figure 9, the two measured SWCCs a are almost identical, and the reason is that the pore distribution of Sample A which is redistributed during the consolidation results in the pore distribution of Sample A is of the same level as that of Sample B after consolidation test. That is, the pore structure of Sample A is the same as that of Sample B. When the pore structures are similar, the consolidation stress will not directly affect the SWCC. Therefore, under the same environmental conditions (e.g., the same suction, the same volume water content, etc.), the consolidation stress only changes the dry density of the sample and redistributes the pore of the sample in order to achieve the same pore distribution between the two samples. So, the direct influence of SWCC changes is the pore distribution.

6.2. Comparison of SWCC Measured by the One-Step Outflow Test after Consolidation.

Sample A is placed into the improved pressure plate extractor for the one-step outflow test. The parameters are inversely calculated by the experimental data and the one-dimensional moisture migration model, and the fitted parameters are shown in Table 3. The fitted parameters in Table 3 are taken into the VG model to fit SWCC of Sample A by the one-step outflow test, and the fitted SWCC is shown in Figure 10. Another curve is the measured SWCC of Sample A in Figure 10. The two fitted SWCCs of Sample A and Sample B are compared and analyzed as shown in Figure 11. In Figure 10, the fitted SWCC of Sample A by the one-step outflow test almost overlaps the

TABLE 3: Fitting parameters of Sample A.

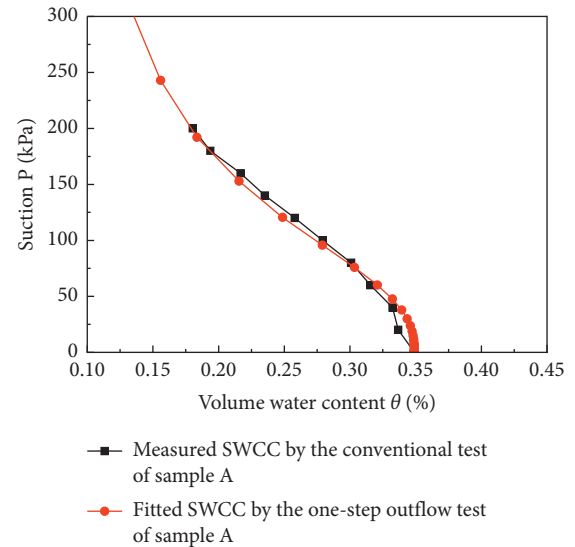| VG model parameter				
A (cm^{-1})	n	m	θr	θs
0.0009	2.20	0.545	0.073	0.349

FIGURE 10: Comparison between fitted SWCC and measured SWCC of Sample A.
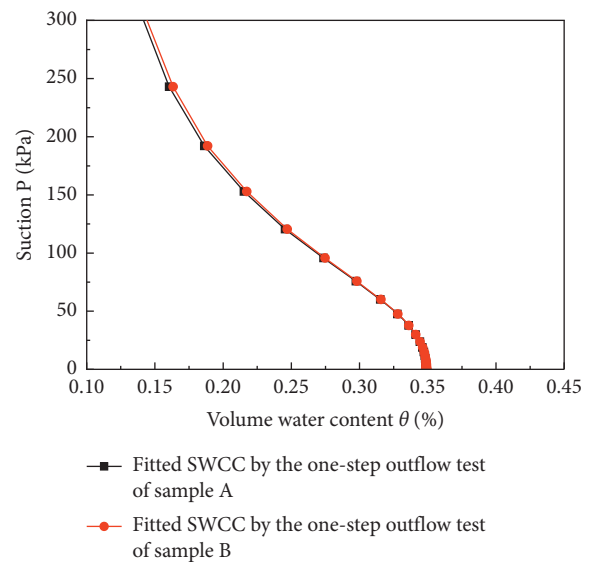

FIGURE 11: Comparison of fitted SWCC in Sample A and Sample B.

measured SWCC by the conventional test. In Figure 11, after the consolidation test, the fitted SWCC of Sample A is almost identical to that of Sample B. It is shown that the dry density and pore distribution of Sample A after consolidation test are similar to those of Sample B. The consolidation test leads to redistribution of pores in Sample A, so that the pore distribution of Sample A is the same as that of Sample

B. Therefore, the two samples also have the same pore distribution, so the two SWCCs are almost identical.

The four SWCCs in Figures 10 and 11 coincide almost completely, which proves that the SWCC is in a close relationship with pore distribution but not a direct relationship with the consolidation pressure. The consolidation pressure only changes the dry density of the sample and redistributes the pore of the sample in order to achieve the same pore distribution between the two samples. The pore distribution is a direct factor affecting the SWCC, which is changed by the consolidation pressure to affect the SWCC, so the consolidation pressure is an indirect factor affecting the SWCC.

7. Conclusion

The original pressure plate extractor in the conventional test takes a long time to measure SWCC. The problem of gas produced by the long loading pressure accumulating at the back of the ceramic plate is difficult to overcome. Therefore, rapid and accurate determination of SWCC is particularly important. From the experimental study on the one-step outflow test with the improved pressure plate extractor, the following conclusions can be drawn:

(1) The fitted SWCC is almost consistent with the measured SWCC, which not only verifies the reliability and practicability of the improved pressure plate extractor but also proves that the one-step outflow method is quick and effective.

(2) The improved pressure plate extractor requires only one step to pressurize, and the operation was simple and convenient. In addition, the improved pressure plate extractor reduces the test error.

(3) For the geometry of SWCC, the geometry of SWCC is directly controlled by pore distribution, but the consolidation pressure is only an indirect way. Firstly, the pore distribution of the sample is redistributed by the consolidation pressure, and then the new pore distribution changes the geometry of SWCC. However, the change of pore distribution is affected by consolidation pressure, so the consolidation pressure is an indirect factor affecting the geometry of SWCC.

Data Availability

The data used to support the results of the study are included within the paper.

Conflicts of Interest

The authors declare that there are no conflicts of interest regarding the publication of this paper.

Acknowledgments

References

[1] W. Xiaoyu, K. Yang, and J. Zheng, "Effect of straw addition on soil infiltration characteristics and model-fitting analysis," *Arabian Journal of Geosciences*, vol. 12, no. 13, 2019.

[2] V. Genuchten, "A closed-form equation for predicting the hydraulic conductivity of unsaturated soils," *Soil Science Society of America Journal*, vol. 44, no. 5, pp. 892–898, 1980.

[3] A. Li, Z. Yue, L. Tham, C. Lee, and K. Law, "Field soil-water characteristics and its engineering implication," *Chinese Journal of Rock Mechanics & Engineering*, vol. 23, no. 6, pp. 969–973, 2004.

[4] D. G. Fredlund, A. Xing, M. D. Fredlund, and S. L. Barbour, "The relationship of the unsaturated soil shear strength to the soil-water characteristic curve," *The Canadian Geotechnical Journal*, vol. 32, no. 3, pp. 440–448, 1995.

[5] C. Wei and M. M. Dewoolkar, "Formulation of capillary hysteresis with internal state variables," *Water Resources Research*, vol. 420, no. 7, pp. 260–273, 2006.

[6] X. Xi, Z. Yin, S. Yang, and C.-Q. Li, "Using artificial neural network to predict the fracture properties of the interfacial transition zone of concrete at the meso-scale," *Engineering Fracture Mechanics*, vol. 242, Article ID 107488, 2021.

[7] D. L. Wang, M. T. Luan, and Q. Yang, "Experimental study on volume change of unsaturated soils and its application to estimation of subsidence," *Journal of Disaster Prevention & Mitigation Engineering*, vol. 27, no. 3, pp. 307–311, 2007.

[8] S. K. Vanapalli, D. G. Fredlund, and D. E. Pufahl, "The relationship between the soil-water characteristic curve and the unsaturated shear strength of a compacted glacial till," *Geotechnical Testing Journal*, vol. 19, no. 3, pp. 259–268, 1996.

[9] G. Babu, R. E. Link, R. S. Rao, and J. Peter, "Evaluation of shear strength functions based on soil water characteristic curves," *Journal of Testing & Evaluation*, vol. 33, no. 6, pp. 461–465, 2005.

[10] D. G. Fredlund, *Soil Mechanics for Unsaturated Soils*, Wiley, Hoboken, NJ, USA, 1993.

[11] J. Jun, "Study on water infiltration pattern into loess subgrade," *Journal of Highway and Transportation Research and Development*, vol. 21, no. 4, pp. 461–465, 2004.

[12] X. Xi, X. Wu, Q. Guo, and M. Cai, "Experimental investigation and numerical simulation on the crack initiation and propagation of rock with pre-existing cracks," *IEEE Access*, vol. 8, pp. 129636–129644, 2020.

[13] T. H. Wang, "Moisture migration in unsaturated loess subgrade," *Chinese Journal of Geotechnical Engineering*, vol. 030, no. 1, pp. 41–45, 2008.

[14] S. G. Sun, Z. H. Chen, Y. Q. Zhu, Y. H. Liu, and L. Wang, "Coordinated ceramic plate extractors and some problems of SWCC test," *Journal of Logistical Engineering University*, vol. 22, (004), 2006.

[15] N. Lu, A. Wayllace, J. Carrera, and W. J. Likos, "Constant flow method for concurrently measuring soil-water characteristic curve and hydraulic conductivity function," *Geotechnical Testing Journal*, vol. 29, no. 3, 12637 pages, 2006.

[16] C. W. Ng and Y. W. Pang, "Experimental investigations of the soil-water characteristics of a volcanic soil," *Canadian Geotechnical Journal*, vol. 37, no. 6, pp. 1252–1264, 2000.

[17] H. Chen, C. F. Wei, R. T. Yan, P. Chen, and P. P. Yi, "On the determination of the soil-water characteristic curve using the

pressure plate extractor," in *Proceedings of the International Symposium on Geoenvironmental Engineering*, Hangzhou, China, September 2010.

[18] P. P. Yi, S. K. Niu, C. F. Wei, and P. Chen, "Dynamic multi-step outflow method for tests on hydraulic properties of unsaturated soils," *Chinese Journal of Geotechnical Engineering*, vol. 38, no. 10, pp. 1797–1801, 2016.

[19] Wang and D. Lin, "Experimental study on soil water characteristic curve of compacted unsaturated soil," *Advanced Materials Research*, vol. 168-170, pp. 1285–1288, 2011.

[20] S. Lee, Y. Jin, S. Woo, and D. H. Shin, "Approximate cost estimating model of eco-type trade for river facility construction using case-based reasoning and genetic algorithms," *KSCE Journal of Civil Engineering*, vol. 17, no. 2, pp. 292–300, 2013.

[21] Y. Dong, "Measurement of suction-stress characteristic curve under drying and wetting conditions," *Geotechnical Testing Journal*, vol. 40, no. 1, Article ID 20160058, 2017.

[22] L. Shao, T. Wen, X. Guo, and X. Sun, "A method for directly measuring the hydraulic conductivity of unsaturated soil," *Geotechnical Testing Journal*, vol. 40, no. 6, Article ID 20160197, 2017.

[23] H. Rahardjo, X. F. Nong, D. T. T. Lee, E. C. Leong, and Y. K. Fong, "Expedited soil-water characteristic curve tests using combined centrifuge and chilled mirror techniques," *Geotechnical Testing Journal*, vol. 41, no. 1, Article ID 20160275, 2017.

[24] A. Adel, Y. Noriyuki, I. Ryohei, H. Masanori, and K. Shuu, "Continuous pressurization method for a rapid determination of the soil water characteristics curve for remolded and undisturbed cohesionless soils - sciencedirect," *Soils and Foundations*, vol. 60, no. 3, pp. 634–647, 2020.

[25] Y. Zhao, T. Wen, L. Shao et al., "Predicting hysteresis loops of the soil water characteristic curve from initial drying," *Soil Science Society of America Journal*, vol. 84, no. 5, 2020.

[26] G. Zheng, L. Shao, X. Guo, and J. Zhang, "Investigation of the mechanical behavior of an unsaturated soil mixture using a digital image measurement system," *European Journal of Environmental and Civil Engineering*, vol. 24, no. 8, 2018.

[27] C. W. W. Ng and Y. W. Pang, "Influence of stress state on soil-water characteristics and slope stability," *Journal of Geotechnical and Geoenvironmental Engineering*, vol. 126, no. 2, pp. 157–166, 2000.

[28] D. a. Sun, D. Sheng, and Y. Xu, "Collapse behaviour of unsaturated compacted soil with different initial densities," *Canadian Geotechnical Journal*, vol. 44, no. 6, pp. 673–686, 2007.

[29] S. Salager, M. Nuth, A. Ferrari, and L. Laloui, "Investigation into water retention behaviour of deformable soils," *Canadian Geotechnical Journal*, vol. 50, no. 2, pp. 200–208, 2013.

[30] Q. Zhai, H. Rahardjo, A. Satyanaga, G. Dai, and Y. Zhuang, "A framework to estimate the soil-water characteristic curve for the soil with different void ratios," *Bulletin of Engineering Geology and the Environment*, vol. 79, no. 4, 2020.

[31] J. Simunek, "The hydrus 1D software package for simulating the one-dimensional movement of water, heat, and multiple solutes in variably saturated porous media," *Hydrus Software*, vol. 68, 2005.

[32] G. MarcelJ. Feike et al., "Rosetta: a computer program for estimating soil hydraulic parameters with hierarchical pedotransfer functions," *Journal of Hydrology*, vol. 251163 pages, 2001.

[33] X. Wang and C. H. Benson, "Leak-free pressure plate extractor for measuring the soil water characteristic curve," *Geotechnical Testing Journal*, vol. 27, no. 2, pp. 163–172, 2004.

[34] D. Gallipoli, S. J. Wheeler, and M. Karstunen, "Modelling the variation of degree of saturation in a deformable unsaturated soil," *Géotechnique*, vol. 53, no. 1, pp. 105–112, 2003.